Data-Driven Control Synthesis using Koopman Operator: A Robust Approach

Mert Eyüboğlu[1], Nathan Powell[2] and Alireza Karimi[3]

***Abstract*— This paper proposes a data-driven control design method for nonlinear systems that builds upon the Koopman operator framework. In particular, the Koopman operator is used to lift the nonlinear dynamics to a higher-dimensional space where the so-called observables evolve linearly. First, an approximate linear time-invariant (LTI) lifted representation of the nonlinear system is obtained. To take into account the residual error, an approximation of the ℓ_2-gain of the error system is computed from data. Based on the obtained model and the ℓ_2-gain bound, a dynamic feedback controller providing robust performance guarantees is synthesized. The controller synthesis method only depends on the frequency response of the LTI approximation; thus, is independent of the lifting dimension. Next, to further reduce the ℓ_2-gain of the error system, a linear parameter-varying (LPV) lifted model is considered. A control design method based on the robust control of the LTI part of dynamics and compensation of the parameter-varying dynamics is proposed. It is shown that the presented control strategy guarantees internal stability of the closed-loop system under the assumption that the parameter-varying dynamics are open-loop BIBO stable while also delivering robust performance guarantees for certain input-output channels through which the parameter-varying dynamics are fully cancelled.**

I. INTRODUCTION

Effective strategies to control nonlinear systems has remained a central topic in the field of control theory. While control methods for linear systems provide strong theoretical guarantees by employing well-understood design tools, the inherent complexities of more general and less structured nonlinear systems pose significant challenges. Consequently, the Koopman operator theory [1] has gained considerable attention in the past decade for its ability to provide a global linear representation of a large class of nonlinear systems. Instead of explicitly examining the evolution of the system states, Koopman operator theory focuses on the evolution of a lifted space of observable functions typically determined by a nonlinear transformation of the states. While the Koopman operator exhibits linearity on this space of observables, the primary concern is that, even for a finite dimensional nonlinear system, the lifted space is generally infinite-dimensional.

In practice this challenge is navigated by approximating the Koopman operator acting on a high-dimensional, yet still finite, set of observable functions. Various algorithms exist to compute tractable approximations. One of the most straightforward and prevalent approximation techniques comes from Extended Dynamics Mode Decomposition (EDMD) [2]. While EDMD has been applied to a wide range of problems for estimation [3], [4] and control [5], [6], establishing rigorous bounds on approximation errors remains an ongoing topic of research [7], [8]. Thus, most of the existing control methods based on the Koopman operator lack guarantees of closed-loop stability.

While the Koopman operator framework has been well-studied for autonomous systems, controller design necessitates the consideration of forced dynamics. Motivated by this, [9] presented the application of this paradigm to systems with inputs. However, a notable concern for Koopman theory in the context of forced systems is the fact that the linearity of the lifted dynamics in observables does not necessarily extend to linearity in the inputs. In light of the firmly established control methodologies for LTI systems, several studies imposed linearity in inputs by restricting the choice of observables to functions that are linear in inputs [5], [6]. However, the validity or consequences of such a restriction on the space of observables for general nonlinear systems is not thoroughly discussed.

It is imperative to acknowledge a broader spectrum of systems characterized by a more general structure, where the lifted model may not inherently exhibit linearity with respect to the system inputs. The work in [10] showed that a valid Koopman representation that is linear in inputs is not guaranteed to exist even in the infinite dimensional case. It is presented that in continuous-time, Koopman lifting results in an LPV representation even for input linear or control-affine nonlinear systems [11]. Iacob et al. [12] extended this to the case of discrete-time systems while also characterizing the approximation error introduced by using an LTI representation instead of an LPV one. These works highlighted the limitations of LTI lifted representations prompting the consideration of less restrictive spaces of observable functions. Bruder et al. [13] discussed the advantages of bilinear lifted models over LTI ones claiming that they strike a compromise between generality and ease of controller design. Sinha et al. [14] presented stabilizing state feedback controller design method for input-affine nonlinear systems using a bilinear representation. More recently, again based on a bilinear representation, Strasser et al. [15] proposed a stabilizing state feedback synthesis method that is applicable for general nonlinear systems by also accounting for the modeling error under a finite-gain assumption.

In this paper, we introduce a data-driven robust control

The authors are with the École Polytechnique Fédérale de Lausanne (EPFL), Institute of Mechanical Engineering, CH-1015 Lausanne, Switzerland (e-mails: mert.eyuboglu@epfl.ch; nathan.powell@epfl.ch; alireza.karimi@epfl.ch

This work has been supported by the Swiss National Science Foundation under NCCR Automation (grant agreement 51NF40 180545).

framework for nonlinear systems based on Koopman lifting. First, we examine the scenario of LTI lifted models. By utilizing the available data that was used for lifting, we also compute an approximation of the ℓ_2-gain of the error system with probabilistic guarantees based on the scenario approach [16]. We then design a dynamic feedback controller that ensures robust performance guarantees in the closed-loop. Our approach utilizes the fixed-structure data-driven controller design method proposed in [17], accommodating mixed $\mathcal{H}_2/\mathcal{H}_\infty$ objectives. As this synthesis method relies solely on the frequency response data of the LTI model, the complexity of the synthesis problem becomes independent of the lifting dimension. This mitigates a primary drawback associated with Koopman lifting for controller synthesis, enabling the use of high-order models and facilitating the design of superior-performing controllers. Next, to further minimize the ℓ_2-gain of the error system, we consider the identification of lifted LPV models. For controller synthesis, we treat the model as a sum of an LTI model and an LPV model. To adress the LTI component, we again synthesize a robust controller following the approach in [17], while we design a compensator for the remaining LPV part. Under the assumption that time-varying part of the lifted dynamics are open-loop bounded-input bounded-output (BIBO) stable, we show that the proposed controller provides internal stability guarantees for the closed-loop system as well as performance guarantees for certain input-output channels.

The rest of this paper is organised as follows, a brief background on Koopman operator theory, EDMD and the employed FRF data based control synthesis method is provided in Section II. In Section III, based on a lifted LTI representation, the linear controller design method with robust performance guarantees is presented. Next, an LPV Koopman representation is considered to alleviate the error and a stabilizing control strategy with LPV compensation is proposed in Section IV. Conclusions and future work are discussed in Section V.

II. Background

In this section, a brief background on Koopman operator theory, data-driven identification of Koopman lifted representations via EDMD and employed frequency response function (FRF) based controller synthesis method is provided.

A. Koopman lifting

Consider the discrete-time nonlinear system,

$$x_{k+1} = f(x_k, u_k), \tag{1}$$

where $x \in \mathcal{X} \subseteq \mathbb{R}^{n_x}$ is the state variable, $u \in \mathcal{U} \subseteq \mathbb{R}^{n_u}$ is the input and $f : \mathcal{X} \times \mathcal{U} \to \mathcal{X}$ is the nonlinear state transition map. The Koopman operator $\mathcal{K}_f : \mathcal{F} \to \mathcal{F}$ is a linear operator that advances an observable function $\phi(x_k, u_k)$ one-step forward in time,

$$\phi(x_{k+1}, u_{k+1}) = \mathcal{K}_f \phi(x_k, u_k) = \phi(f(x_k, u_k), u_{k+1}). \tag{2}$$

where $\mathcal{F}$ is a Banach space of observable functions that is invariant under the action of the Koopman operator. Therefore, the main idea behind the Koopman framework is to express the system dynamics in terms of the lifted states of observable functions instead of the state variable x itself. By doing so, the Koopman operator $\mathcal{K}$ globally maps the nonlinear dynamics in the state space to linear dynamics in the lifted space of observables. Readers can refer to [1], [18]–[21] for more details on Koopman operator theory.

In general, the Koopman operator acts on an infinite-dimensional space of functions. In practice, however, a finite-dimensional approximation of the Koopman operator must be employed. To achieve so, a finite set of regressors or observable functions $\mathcal{D} = \{\phi_j\}_{j=1}^{d}$ called a dictionary is considered. Then, the approximate Koopman operator $\mathcal{K}_\Phi$ defined on the d dimensional space of observables $\mathcal{F}_\Phi \subset \mathcal{F}$ propagates $\Phi(x) = \begin{bmatrix}\phi_1(x) & \dots & \phi_N(x)\end{bmatrix}^T$ forward in time,

$$\Phi(x_{k+1}) = \mathcal{K}_\Phi \Phi(x_k) + r_{k,\Phi}, \tag{3}$$

with $r_{k,\Phi} := r_{k,\Phi}(x_k, u_k)$ being the truncation error that is also dependent on the choice of dictionary.

Given its maturity and intuitive structure, identifying an LTI model is often times desirable for control design. Identifying an LTI system is realizable by restricting the dictionary of observables to the form,

$$\Phi(x_k, u_k) = \begin{bmatrix}\Phi_x(x_k, u_k) & \Phi_u(x_k, u_k)\end{bmatrix}^T = \begin{bmatrix}\Phi_x(x_k) & u_k\end{bmatrix}^T, \tag{4}$$

yielding,

$$\Phi_x(x_{k+1}) = A_\Phi \Phi_x(x_k) + B_\Phi u_k + \varepsilon_{k,\Phi}, \tag{5}$$

where the identified system matrix A_Φ, control influence B_Φ and residual error $\varepsilon_{k,\Phi}$ depend on the choice of regressors in Φ. While the aforementioned approach facilitates the application of established control techniques for LTI systems, it comes with a notable drawback. Iacob et al. [12] demonstrated that, even in cases of nonlinear systems with linear inputs, the exact lifted representation remains nonlinear with respect to inputs. This trade-off becomes evident: imposing a linear input structure on the model for the sake of simplifying control inevitably leads to increased residual modeling error $\varepsilon_{k,\Phi}$.

In order to reduce this error while still arriving at a model that is desirable for control design, $\Phi_u(x_k, u_k) = \Phi_u(x_k)u_k$ can be chosen. This delivers an LPV model in the form,

$$\Phi_x(x_{k+1}) = A_\Phi \Phi_x(x_k) + B_\Phi \Phi_u(x_k) u_k + \varepsilon_{k,\Phi}. \tag{6}$$

Some approaches [13]–[15] consider the specific case where $\Phi_u(x_k) = \Phi_x(x_k)$ which results in a bilinear model that is a relatively desirable form for control design. However, this work considers the more general case (6) resulting in an LPV system where the parameter dependence is only embedded in to the input matrix $\bar{B}(x_k) = B\Phi_u(x_k)$.

B. Extended dynamic mode decomposition

Here we briefly summarize the EDMD algorithm [2] that enables the computation of the A_Φ and B_Φ matrices in (6) by solving a least-squares problem. Based on a set of data

trajectories with N samples $\{x_k, u_k\}_{k=0}^{N-1}$ and a selected dictionary of observable functions $\mathcal{D}$, the matrices

$$X := \begin{bmatrix}\Phi_x(x_0) & \dots & \Phi_x(x_{N-2})\end{bmatrix},$$
$$X^+ := \begin{bmatrix}\Phi_x(x_1) & \dots & \Phi_x(x_{N-1})\end{bmatrix},$$

and

$$U := \begin{bmatrix}\Phi_u(x_0)u_0 & \dots & \Phi_u(x_{N-2})u_{N-2}\end{bmatrix},$$

are constructed. Then, the matrices A_Φ and B_Φ in (6) can be obtained by solving,

$$\min_{A,B} \quad \left\| X^+ - \begin{bmatrix}A_\Phi & B_\Phi\end{bmatrix}\begin{bmatrix}X\\U\end{bmatrix}\right\| \tag{7}$$

which has the ℓ_2-optimal solution $\begin{bmatrix}A_\Phi & B_\Phi\end{bmatrix} = X^+\begin{bmatrix}X\\U\end{bmatrix}^\dagger$. This yields the optimal matrices satisfying the system dynamics (6) such that $\|\varepsilon_{k,\Phi}\|_2$ is minimized. Note that again by setting $\Phi_u(x_k) = 1$, an LTI model as in (5) can be obtained.

C. FRF based controller synthesis algorithm

The problem of mixed sensitivity controller synthesis using only frequency domain data is addressed in [17]. Given the FRF $G(e^{jw})$ of an LTI system and a structured controller $K = XY^{-1}$ with polynomial matrices $X(z)$ and $Y(z)$, the algorithm minimizes the norm of a mixed-sensitivity problem. For illustration purposes we can consider the basic problem,

$$\min_K \|W_1\mathcal{S}\|_\infty \tag{8}$$

where W_1 is a weighting filter and $\mathcal{S} = (I + GK)^{-1}$ is the sensitivity function. Assuming that an initial stabilizing controller $K_c = X_cY_c^{-1}$ is known, a stabilizing controller K, which delivers a sub-optimal solution of (8), can be obtained by solving,

$$\begin{aligned}&\min_K \quad \gamma\\ &s.t. \quad \begin{bmatrix}P^*P_c + P_c^*P - P_c^*P_c & (W_1Y)^*\\ (W_1Y) & \gamma I\end{bmatrix} > 0 \quad \forall\omega\in\Omega,\end{aligned} \tag{9}$$

where $\Omega = (-\pi/T_s, \pi/T_s]$ with T_s the sampling period, $P = Y + GX$ and $P_c = Y_c + GX_c$. Note that the optimization problem (9), depends only on the frequency response data of the system. Thus, the complexity of the problem depends only on the input-output dimensions of system G while it remains independent of its number of states. See [17] for further details and the stability proof.

III. Linear Feedback Controller Design

We consider the general nonlinear system with inputs (1) and our goal is to design a stabilizing controller with performance guarantees by only using the data $\{x_k, u_k\}_{k=0}^{N-1}$ collected from the system. Using the available data we first identify a lifted LTI representation (5) of the system considering a set of appropriate observable functions (4). We compute the system matrices in (5) by following the EDMD algorithm. Then, we select the output of the lifted system as a subset of the observables that we would like the controller to act on, i.e. $\bar{y} = C_\Phi\Phi(x) = \begin{bmatrix}I & 0\end{bmatrix}\Phi(x)$.

Since, $\bar{y}$ does not correspond to the true output of the system, we also identify a mapping $\bar{C}_\Phi$ from $\bar{y}$ to the output of the true system by solving the following least-squares problem,

$$\min_{\bar{C}} \quad \left\|Y - \bar{C}_\Phi\bar{Y}\right\|, \tag{10}$$

where $\bar{Y} = \begin{bmatrix}\bar{y}(x_0) & \dots & \bar{y}(x_{N-1})\end{bmatrix}$. The resulting approximated output $\hat{y}$ is the best projection of the true output y on the span of $\bar{y}$ in a least squares sense, i.e. $y \approx \hat{y} = \bar{C}_\Phi\bar{y}$.

Remark 1: It is a common choice to include the true output of the system in the set of observable functions such that $\Phi(x) = \begin{bmatrix}y(x) & \phi_1(x) & \dots & \phi_N(x)\end{bmatrix}$ as well in the outputs of the lifted model $\bar{y} = \begin{bmatrix}I & 0\end{bmatrix}\Phi(x)$. This makes the mapping from $\bar{y}$ to the true output trivial such that $\hat{y} = \bar{C}_\Phi\bar{y} = \begin{bmatrix}I & 0\end{bmatrix}\bar{y}$. We also consider this case in the rest of the paper for the sake of simplicity.

As a result, we obtain a nominal LTI model G_0,

$$G_0 : \begin{cases} z_{k+1} &= A_\Phi z_k + B_\Phi u_k,\\ \bar{y}_k &= C_\Phi z_k,\end{cases} \tag{11}$$

with $z_k \approx \Phi_x(x_k)$, and an error system Δ that we treat as uncertainty,

$$\Delta : \begin{cases}\varepsilon_{k+1} = \Phi(x_{k+1}) - z_{k+1},\\ e_k = C_\Phi\varepsilon_k,\end{cases} \tag{12}$$

such that $G = \bar{C}_\Phi(G_0 + \Delta)$ where G represents the true nonlinear system. The block diagram representation of the resulting closed-loop system is presented in Fig. 1.

In order to design a controller with performance guarantees for the closed-loop system in Fig. 1, the ℓ_2-gain of Δ must be characterized from data such that the well known small-gain theorem can be employed for robust controller synthesis.

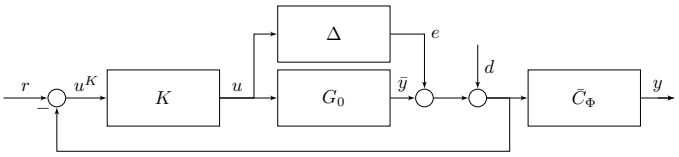

Fig. 1. Block diagram of the closed-loop system with an LTI Koopman representation.

A. Lower bound on ℓ_2-gain of error system

We rewrite the dynamics (12) of the error system Δ as,

$$\Delta : \begin{cases}\varepsilon_{k+1} = \Phi(x_{k+1}) - A_\Phi z_k - B_\Phi u_k,\\ e_k = C_\Phi\varepsilon_k,\end{cases} \tag{13}$$

with $\varepsilon_0 = 0$ such that the true system and the LTI representation have the same initial conditions.

Definition 1: Let $\gamma \geq 0$, the error system Δ (13) is said to have linear ℓ_2-gain less than or equal to γ if,

$$\sum_{k=0}^{N-1}\|e_k\|^2 \leq \gamma^2\sum_{k=0}^{N-1}\|u_k\|^2 + \beta(|\varepsilon_0|), \tag{14}$$

for some $\mathcal{K}$-function β for all $N \geq 1$ and all $u \in \ell_2[1, N]$.

In Definition 1, the $\beta(|\varepsilon_0|)$ term represents the energy stored in the system due to initial conditions. Since $\beta(|\varepsilon_0|) \geq 0$, a suboptimal ℓ_2-gain $\hat{\gamma}$ of Δ can be obtained by solving the semi-infinite problem,

$$\begin{aligned} \min_{\hat{\gamma} \geq 0} \quad & \hat{\gamma} \\ s.t. \quad & \sum_{k=0}^{N-1} \|e_k\|^2 \leq \hat{\gamma}^2 \sum_{k=0}^{N-1} \|u_k\|^2, \quad \forall u \neq 0 \in \ell_2[1, N], \end{aligned} \tag{15}$$

$\forall N \geq 1$. Since (15) is a convex problem wit infinitely many constraints, we aim for obtaining a super-optimal solution $\bar{\gamma} \leq \hat{\gamma}$ to (15) by making use the available data that we have also used for Koopman lifting.

Using the available M data trajectories that were used for EDMD, we first compute the corresponding M trajectories of $\{\{e_k^m\}_{k=0}^{N-1}\}_{m=1}^{M}$ according to (13). Then, using these trajectories we compute an approximate ℓ_2-gain of Δ by solving,

$$\begin{aligned} \min_{\bar{\gamma} \geq 0} \quad & \bar{\gamma} \\ s.t. \quad & \sum_{k=0}^{N-1} \|e_k^m\|^2 \leq \bar{\gamma}^2 \sum_{k=0}^{N-1} \|u_k^m\|^2, \quad \forall m \in [1, M]. \end{aligned} \tag{16}$$

Assumption 1: Let the available data trajectories $\{\{x_k^m, u_k^m\}_{k=0}^{N-1}\}_{m=1}^{M}$ be such that, for all $m = [1, M]$ and $k = [0, N-1]$, each input sample u_k^m are randomly chosen independent identically distributed (i.i.d.) samples from a set of admissible inputs $\mathcal{U} \subset \mathbb{R}^{n_u}$.

Assumption 1 implies that each input trajectory $\{u^m\}_{m=1}^{M}$ is also an i.i.d. sample from the set $u \in \ell_2^N$. Thus, by solving (16) we replace the infinite number of constraints in (15) by M randomly chosen i.i.d. constraints. Then, by the scenario approach [16], if,

$$M \geq \frac{2}{\epsilon}\left(\ln \frac{1}{\beta} + 1\right), \tag{17}$$

with probability no smaller than $1 - \beta$, $\bar{\gamma}$ satisfies all constraints in (15) but at most an ϵ-fraction. For example consider we have $M = 2000$ system trajectories with $N = 100$ samples where $e_k \in \mathbb{R}^2$, having a violation probability greater than $\epsilon = 0.01$ has a probability less than 1.2341×10^{-4} while this upper bound exponentially goes to 0 with M.

B. Controller Synthesis

Considering $\bar{\gamma}$ obtained by solving (16) as an accurate approximate bound on the ℓ_2-gain of Δ and the lifted LTI representation (11) as a nominal model, we can synthesize a controller by following the approach of [17]. The schematic of the resulting closed-loop system with robust performance guarantees is presented in Fig. 1. The benefits of using this FRF data based controller synthesis algorithm within Koopman framework are twofold:

- Since the method only uses the input-output FRF data for the synthesis, the complexity of the controller synthesis problem is independent of the lifting dimension.
- As the algorithm allows for structured controller synthesis, the order of the resulting controller can also be chosen independently from the lifting dimension.

Both of these aspects allow for the usage of high order Koopman representations without resulting in computational or implementation issues.

C. Numerical example

In this section, we illustrate our approach with a simple simulation example. We consider the forced nonlinear Van der Pol oscillator,

$$\dot{x}_1 = x_2, \tag{18}$$

$$\dot{x}_2 = (1 - x_1^2)x_2 - x_1 + u. \tag{19}$$

We first obtain the discrete-time dynamics by forward Euler discretization with step time $T_s = 0.005s$. For data generation we consider uniformly distributed initial conditions inside a box $x_0^m \in [-1.5, 1.5]^2$ and uniformly distributed random inputs $u_k^m \in [-1.5, 1.5]$. We generate $M = 3000$ data trajectories of length $N = 100$ by simulating the discretized model. For EDMD, we consider the observables $\Phi(x) = \begin{bmatrix} x_1 & x_2 & x_1^2 & x_1x_2 & x_1^2x_2 & u \end{bmatrix}^T$ resulting in a 5 dimensional lifted LTI representation. The input dimension of the controller K is chosen as 3 with $C_\Phi = \begin{bmatrix} I^{3\times 3} & 0^{3\times 2} \end{bmatrix}$ such that the controller is acting on the subset of obervables $\{x_1, x_2, x_1^2\}$. Then, by solving (16), we obtain the lower bound on ℓ_2-gain of Δ as $\bar{\gamma} = 0.4271$ where having a violation probability greater than $\epsilon = 0.01$ is guaranteed to be less than 8.3153×10^{-7} by the scenario approach. Lastly, the controller is synthesized by employing the algorithm in [17] where,

$$\begin{aligned} \min_{K} \quad & \left\|W_1(I + G_0K)^{-1}\right\|_2 \\ s.t. \quad & \left\|W_2K(I + G_0K)^{-1}\right\|_\infty < 1, \end{aligned} \tag{20}$$

is solved based on the FRF of the lifted representation where $W_1 = \begin{bmatrix} 1 & 0 & 0 \end{bmatrix}$ and $W_2 = \bar{\gamma}$ and K is a first-order dynamic controller. As a result the controller is obtained in state-space form as,

$$\begin{aligned} x_{k+1}^K &= 0.624x_k^K + \begin{bmatrix} -0.4514 & 0.6046 & -0.05328 \end{bmatrix} u_k^K, \\ y_k^K &= u_k = 0.7564x_k^K + \begin{bmatrix} 2.093 & 0.6543 & 0.141 \end{bmatrix} u_k^K, \end{aligned}$$

The closed-loop trajectory of the true system states with the resulting controller simulated from the initial condition $x_0 = [1, -0.6]$ with $r = d = 0$ is presented in Fig. 2. The evolution of the system states in the state-space is also plotted in Fig. 3. For comparison, we also synthesize the LQR controller for cost matrices $Q = diag(\begin{bmatrix} 1 & 0 & 0 & 0 & 0 \end{bmatrix})$ and $R = 1$ however it is observed that the resulting controller fails to stabilize the true system which showcases the importance of the consideration of Koopman lifting errors.

IV. Output Feedback Controller Design with LPV compensation

While LTI Koopman models are often used in the literature due to their convenience, it is shown that a valid Koopman

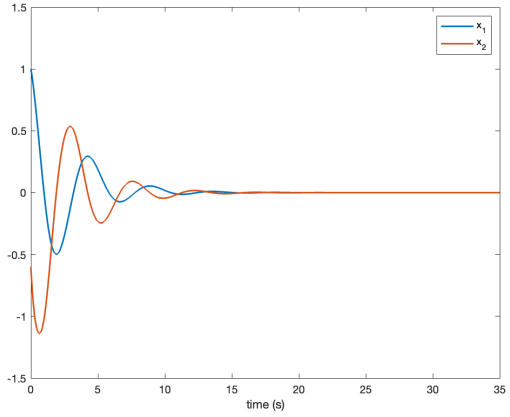

Fig. 2. Closed-loop trajectory with $x_0 = [1, -0.6]$.

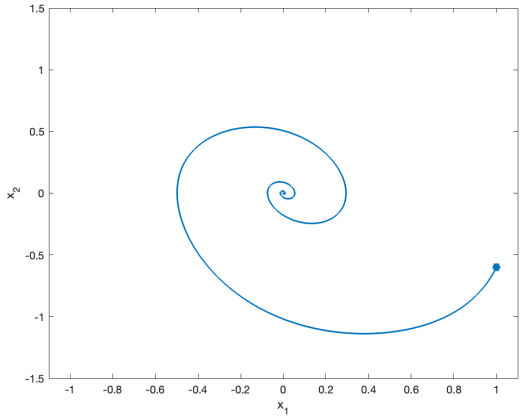

Fig. 3. Closed-loop trajectory with $x_0 = [1, -0.6]$.

representation is not guaranteed to exist in the LTI form [10]. It is shown in [11], [12] that even nonlinear systems that are linear in inputs do not assume an LTI form when Koopman lifting is performed, either in the continous-time or the discrete-time cases. Thus, in order to reduce the error bounds such representations are yielding, we consider Koopman lifted LPV representations in this section.

We first employ the EDMD algorithm by considering a dictionary of lifting functions structured as

$$\begin{aligned}\Phi(x_k, u_k) &= \begin{bmatrix}\Phi_x(x_k, u_k) & \Phi_u(x_k, u_k)\end{bmatrix}^T \\ &= \begin{bmatrix}\Phi_x(x_k) & \Phi_u(x_k)u_k\end{bmatrix}^T \\ &= \begin{bmatrix}\Phi_x(x_k) & u_k & \hat{\Phi}_u(x_k)u_k\end{bmatrix}^T\end{aligned} \tag{21}$$

yielding an LPV lifted representation as in (6). Furthermore, we select $\Phi_x(x) = \begin{bmatrix}y(x) & \phi_1(x) & \dots & \phi_N(x)\end{bmatrix}$, i.e.

$$\hat{y} = \bar{C}_\Phi \bar{y} = \bar{C}_\Phi C_\Phi \Phi_x(x) = \begin{bmatrix}I & 0\end{bmatrix} \Phi_x(x),$$

resulting in the following LPV representation,

$$\hat{G}: \begin{cases} z_{k+1} = A_\Phi z_k + \hat{B}_{0,\Phi} u_k + \hat{B}_{1,\Phi}\Phi_u(x_k)u_k, \\ \bar{y}_k = C_\Phi z_k. \end{cases} \tag{22}$$

where $z_k \approx \Phi(x)$. Next, we rewrite the lifted system $\hat{G}$ (22) as the sum of an LTI and an LPV system as $\hat{G} = G_0 + G_1(\Phi_u(x_k))$ with,

$$G_0: \begin{cases} z_{0,k+1} = A_\Phi z_{0,k} + B_{0,\Phi} u_k, \\ \bar{y}_{0,k} = C_\Phi z_{0,k}, \end{cases} \tag{23}$$

$$G_1(\Phi_u(x_k)): \begin{cases} z_{1,k+1} = A_\Phi z_{1,k} + B_{1,\Phi}(\Phi_u(x_k))u_k, \\ \bar{y}_{1,k} = C_\Phi z_{1,k}. \end{cases} \tag{24}$$

where $B_{0,\Phi} = \hat{B}_{0,\Phi}$, $B_{1,\Phi}(\Phi_u(x_k)) = \hat{B}_{1,\Phi}\Phi_u(x_k)$ yielding $z_k = z_{0,k} + z_{1,k}$ and $\bar{y}_k = \bar{y}_{0,k} + \bar{y}_{1,k}$. Then, the resulting residual error system to be treated as uncertainty is,

$$\Delta: \begin{cases} \varepsilon_{k+1} = \Phi(x_{k+1}) - A_\Phi z_k - B_{0,\Phi} u_k - B_{1,\Phi}(\Phi_u(x_k))u_k, \\ e_k = C_\Phi \varepsilon_k, \end{cases} \tag{25}$$

such that $G = G_0 + G_1(\Phi_u(x_k)) + \Delta$, where G represents the true nonlinear system. We again obtain a super-optimal ℓ_2-gain of Δ by solving (16) while probabilistic guarantees on constraint violation can again be derived by the scenario approach.

Theorem 1: If $G_1(\Phi_u(x_k))$ is bounded-input bounded-output (BIBO) stable and the feedback controller K robustly stabilizes G_0 with respect to the uncertainty,

$$\Delta = G - G_0 - G_1,$$

the closed-loop system in Fig. 4 is also internally stable.

Proof: Since K robustly stabilizes G_0, the controller output u is bounded for any bounded external input. In other words, it is guaranteed that the input of $G_1(\Phi_u(x_k))$ is a bounded signal. Thus, as long as $G_1(\Phi_u(x_k))$ is already a BIBO stable system, all the internal signals of the closed-loop system in Fig. 4 remain bounded for any external input such that the closed-loop system is BIBO stable. ■

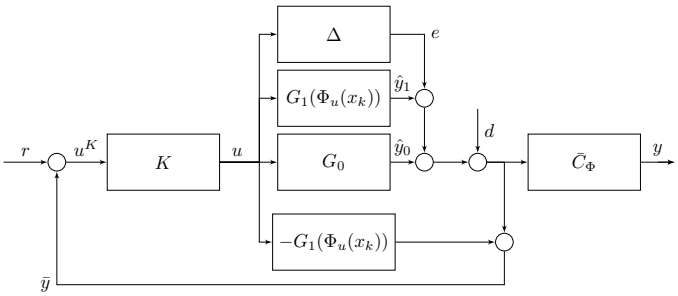

Fig. 4. Block diagram of the closed-loop system with LPV controller.

Based on Theorem 1, we synthesize the controller K for the LTI part G_0 of the lifted representation by employing the method in [17]. It should be noted that since $-G_1(\Phi_u(x_k))$ is also a part of the controller, the final controller to be implemented is also parameter-dependent, which requires the measurement of the system outputs as well as the absence of any unmeasured disturbances on the input of the system.

Remark 2: It should be noted that in this case, we can give performance guarantees for only certain input-output

channels on which $G_1(\Phi_u(x_k))$ has no effect. The effect of $G_1(\Phi_u(x_k))$ persists through the paths from any external input to the true output of the system y. Thus, no performance guarantees on y can be provided. Still, one may identify G_0 as the best linear approximation (BLA) of the nonlinear system and optimize the performance of $\bar{y}$ during the controller design. Even though this would not deliver any performance guarantees for y, if $G_1(\Phi_u(x_k))$ is small when compared to G_0, the performance of the closed-loop system can still be improved. On the other hand, the effect of $G_1(\Phi_u(x_k))$ is fully canceled from any external input to u^K and u, for which it is possible to give performance guarantees.

A. Numerical examples

To highlight the benefits of LPV lifted representations and to illustrate our control approach, we consider a bilinear DC motor example. After a coordinate shift to make the origin a fixed point [22], the system dynamics can be expressed as,

$$\dot{x}_1 = -\frac{R_a}{L_a}x_1 - \frac{k_m}{L_a}x_2 u + \frac{k_m \tau_1}{L_a B}u, \tag{26}$$

$$\dot{x}_2 = -\frac{B}{J}x_2 + \frac{k_m}{J}x_1 u + \frac{k_m u_a}{J R_a}u, \tag{27}$$

where x_1 is the rotor current, x_2 the angular velocity, and the control input u is the stator current. The parameters are $L_a = 0.314, R_a = 12.345, k_m = 0.253, J = 0.00441, B = 0.00732, \tau_1 = 1.47, u_a = 60$. We obtain the discrete-time dynamics by the 4^{th}-order Runge-Kutta method for a step time of $T_s = 0.01s$. For data generation, we consider uniformly distributed initial conditions inside a unit box $x_0^m \in [-1, 1]^2$ and uniformly distributed random inputs $u_k^m \in [-1, 1]$. We generate $M = 2000$ data trajectories of length $N = 200$ by simulating the discretized model.

For Koopman lifting, we first consider the observables consisting of the system states and 20 radial basis functions $\Phi_0(x) = \begin{bmatrix} x_1 & x_2 & \phi_1(x) & \dots & \phi_{20}(x) & u \end{bmatrix}^T$ where $\phi_i(x)$ are Gaussian radial basis functions with randomly generated centers inside the unit box $[-1, 1]$. By employing the EDMD algorithm, we obtain the state transition matrix A_0 and input matrix B_0 yielding an LTI representation G_0 with 22 states. Next, to obtain an LPV representation, we consider

$$\Phi_1(x) = \begin{bmatrix} x_1 & x_2 & \phi_1(x) & \dots & \phi_2(x) & u & x_1 u & x_2 u \end{bmatrix}^T$$

and solve,

$$\min_{B_1} \quad \left\| X^+ - \begin{bmatrix} A_0 & B_0 & B_1 \end{bmatrix} \begin{bmatrix} X \\ U \end{bmatrix} \right\| \tag{28}$$

for the fixed A_0 and B_0 corresponding to the LTI dynamics G_0. This yields a model $\hat{G} = G_0 + G_1$ as in (22)-(24). By using this two-step EDMD, we aim to cover as much of the system behavior by G_0, since we can only deliver performance guarantees for the purely LTI part, and use the LPV part G_1 to reduce the residual error.

We select $C = \begin{bmatrix} I^{2\times 2} & 0^{2\times 20} \end{bmatrix}$ such that the controller is only acting on the true system states x_1, x_2. When only the linear model G_0 is considered, we obtain the approximate ℓ_2-gain of the error system as $\bar{\gamma}_0 = 32.09106$. On the other hand, when the LPV model $\hat{G} = G_0 + G_1$ is considered, we obtain $\bar{\gamma} = 25.00404$. This significant reduction of the approximated ℓ_2-gain of the error system clearly demonstrates the benefit of using an LPV representation since it reduces the required robustness margin for controller synthesis, alleviating conservatism in performance. To further illustrate the higher accuracy of the LPV representation, the trajectories of x_1 and x_2 for G_0, $\hat{G}$, and the true system G for a square-wave input signal u with amplitude 1 and period 10 seconds are presented in Fig. 5.

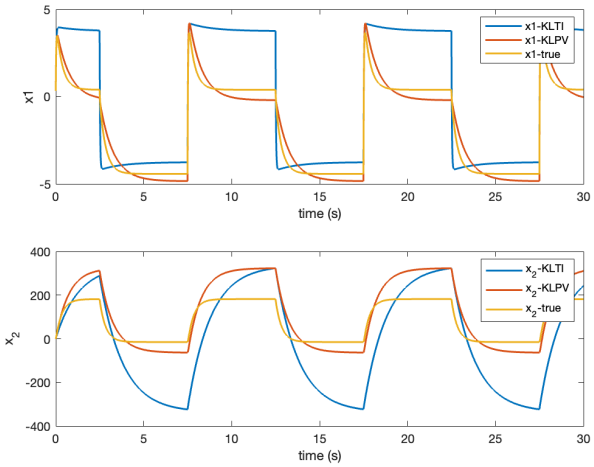

Fig. 5. Open-loop simulation of the DC motor and its LTI and LPV representations.

Lastly, the controller K is synthesized by employing the algorithm in [17] where,

$$\begin{aligned} \min_{K} \quad & \left\| W_1 (I + G_0 K)^{-1} \right\|_2 \\ s.t. \quad & \left\| W_2 K (I + G_0 K)^{-1} \right\|_\infty < 1, \end{aligned} \tag{29}$$

is solved based on the FRF of the lifted representation where $W_1 = I^{2\times 2}$ and $W_2 = \bar{\gamma}$ and K is a second-order dynamic controller. As a result, the controller is obtained in state-space form as,

$$x_{k+1}^K = \begin{bmatrix} 0.465 & 0.196 \\ -0.196 & 0.8635 \end{bmatrix} x_k^K + \begin{bmatrix} -0.001455 & -0.00266 \\ -0.0001084 & -0.0002175 \end{bmatrix} u_k^K,$$

$$y_k^K = \begin{bmatrix} 0.003032 & -0.0002429 \end{bmatrix} x_k^K + \begin{bmatrix} 6.574 \times 10^{-6} & 1.204 \times 10^{-5} \end{bmatrix} u_k^K.$$

The trajectory of the true system, initialized with $x_0 = [-10, 10]$, in a closed-loop scheme using the resulting controller as shown in Fig. 4, with $r = d = 0$, is presented in Fig. 6.

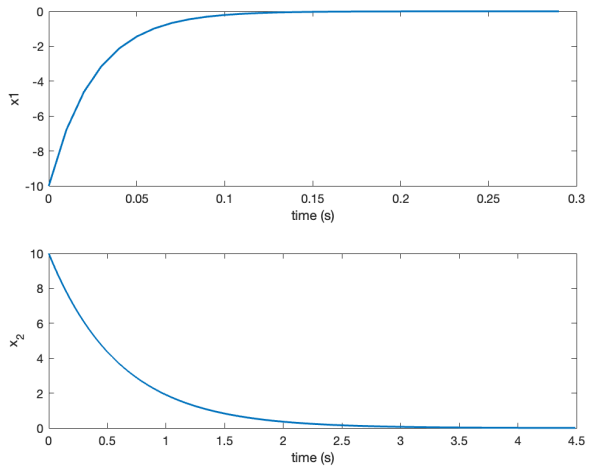

Fig. 6. Closed-loop state trajectories of the bilinear DC motor starting from $x_0 = [-10, 10]^T$

V. Conclusion

In this paper, we presented a data-driven control framework for nonlinear systems exploiting the Koopman operator's ability to represent a nonlinear system as a linear one in a higher-dimensional space. First, the case of LTI lifted models is considered, where we computed an approximate ℓ_2-gain of the error system with probabilistic guarantees based on available data. Synthesizing a linear output feedback controller using a fixed-structure data-driven design method, we achieved robust performance guarantees. A notable advantage of our approach is its independence from the dimension of the Koopman lifting, making it feasible to handle high-order models that contribute to reducing the ℓ_2-gain of the error system. Next, we extended our framework to incorporate LPV models obtained through Koopman lifting. We successfully designed a controller that treats the LPV model as a combination of LTI and LPV components. This approach allowed us to utilize the stability properties of the LTI part while efficiently compensating for the remaining LPV dynamics. Notably, the stability guarantees were maintained under the BIBO stability assumption of the open-loop parameter-varying dynamics. Our methodology contributes to addressing the challenge of data-driven nonlinear control by bridging the gap between the Koopman operator framework and robust control synthesis.

Future work will focus on a more precise characterization of the ℓ_2-gain of the error system from data and providing robust performance guarantees also for the case of LPV lifted representations. Furthermore, refining the approximation techniques for the Koopman operator and the application of this framework to practical examples remain interesting avenues for research.

References

[1] B. O. Koopman, "Hamiltonian systems and transformation in Hilbert space," Proc. Nat. Acad. Sci. United States America, vol. 17, no. 5, pp. 315–318, 1931.

[2] M. O. Williams, I. G. Kevrekidis, and C. W. Rowley, "A data-driven approximation of the Koopman operator: Extending dynamic mode decomposition," J. Nonlinear Sci., vol. 25, no. 6, pp. 1307–1346, 2015.

[3] A. Surana, "Koopman operator based observer synthesis for control-affine nonlinear systems," in Proc. 55th IEEE Conf. Decision and Control, 2016, pp. 6492–6499.

[4] A. Surana and A. Banaszuk, "Linear observer synthesis for non- linear systems using Koopman operator framework," IFAC-PapersOnLine, vol. 49, no. 18, pp. 716–723, 2016.

[5] M.Korda, and I.Mezić, "Linear predictors for nonlinear dynamical systems: Koopman operator meets model predictive control," Automatica, vol. 93, pp. 149–160, 2018.

[6] D. Bruder, B. Gillespie, D. Remy, and R. Vasudevan, "Modeling and control of soft robots using the Koopman operator and model predictive control," Rob. Sci. Syst., 2019.

[7] F. Nüske, S. Peitz, F. Philipp, M. Schaller, and K. Worthmann, "Finite-data error bounds for Koopman-based prediction and control," Journal of Nonlinear Science, vol. 33, pp. 14, 2022.

[8] C. Zhang, and E. Zuazua. "A quantitative analysis of Koopman operator methods for system identi- fication and predictions," Comptes Rendus. Mécanique, Online first, pp. 1-3, 2023.

[9] J. L. Proctor, S. L. Brunton, and J. N. Kutz, "Generalizing Koopman theory to allow for inputs and control," SIAM J. Appl. Dyn. Syst., vol. 17, no. 1, pp. 909–930, 2018.

[10] C. Bakker, S. Rosenthal, and K. E. Nowak "Koopman representations of dynamic systems with control," arXiv preprint arXiv:1908.02233, 2019.

[11] E. Kaiser, J. N. Kutz, and S. L. Brunton, "Data-driven approximations of dynamical systems operators for control. In The Koopman Operator in Systems and Control: Concepts, Methodologies, and Applications," pp. 197–234, Springer International Publishing, 2020.

[12] L. C. Iacob, R. Tóth, and M. Schoukens, "Koopman Form of Nonlinear Systems with Inputs," 2022, arXiv:2207.12132.

[13] D. Bruder, X. Fu, and R. Vasudevan, "Advantages of bilinear Koopman realizations for the modeling and control of systems with unknown dynamics," IEEE Robot. Autom. Lett., vol. 6, no. 3, pp. 4369–4376, 2021.

[14] S. Sinha, S. P. Nandanoori, J. Drgona, and D. Vrabie, "Data-driven stabilization of discrete-time control-affine nonlinear systems: A Koopman operator approach," in Proc. IEEE European Control Conference (ECC), 2022.

[15] R. Strässer, J. Berberich, and F. Allgöwer, "Robust data-driven control for nonlinear systems using the Koopman operator," arXiv:2304.03519, 2023.

[16] G. C. Calafiore and M. C. Campi, "The scenario approach to robust control design," in IEEE Transactions on Automatic Control, vol. 51, no. 5, pp. 742-753, May 2006.

[17] A. Karimi and C. Kammer, "A data-driven approach to robust control of multivariable systems by convex optimization," Automatica, vol. 85, pp. 227–233, 2017.

[18] M. Budišić, R. Mohr, and I. Mezić, "Applied Koopmanism," Chaos, vol. 22, no. 4, pp. 047 510–047 510, 2012.

[19] I. Mezić, "Spectral properties of dynamical systems, model reduction and decompositions," Nonlinear Dynamics, vol. 41, no. 1-3, pp. 309–325, 2005.

[20] P. Bevanda, S. Sosnowski, and S. Hirche, "Koopman operator dynamical models: Learning, analysis and control," Annu. Rev. Control, vol. 52, pp. 197–212, Sep. 2021.

[21] S. L. Brunton, M. Budišić, E.Kaiser, and J. N. Kutz, "Modern koopman theory for dynamical systems," 2021, arXiv:2102.12086.

[22] A. Pal and T. He, "A Robust Dual-loop Control for Finite-dimensional Koopman Model of Nonlinear Dynamical Systems," 2023 American Control Conference (ACC), San Diego, CA, USA, 2023, pp. 3883-3888.